

A Comparison of Shuttling Mechanisms in Two Constitutionally Isomeric Bistable Rotaxane-Based Sunlight-Powered Nanomotors

Vincenzo Balzani,^A Miguel Clemente-León,^{A,C} Alberto Credi,^A Monica Semeraro,^A Margherita Venturi,^{A,E} Hsian-Rong Tseng,^{B,D} Sabine Wenger,^B Sourav Saha,^B and J. Fraser Stoddart^{B,E}

^A Dipartimento di Chimica ‘G. Ciamician’, Università di Bologna, 40126 Bologna, Italy.

^B The California NanoSystems Institute and the Department of Chemistry and Biochemistry, University of California, Los Angeles CA 90095-1569, USA.

^C Current address: Instituto de Ciencia Molecular, Universidad de Valencia, 46100 Burjassot, Spain.

^D Current address: Department of Molecular and Medical Pharmacology and The Crump Institute for Molecular Imaging, University of California, Los Angeles CA 90095, USA.

^E Corresponding authors. Email: margherita.venturi@unibo.it; stoddart@chem.ucla.edu

To find out how best to optimize shuttling of the macrocycle in a particular class of photochemically driven molecular abacus, which has the molecular structure of **BR-I**⁶⁺ in its Mark **I** prototype (Ashton et al., *Chem. Eur. J.* **2000**, *6*, 3558), we have synthesized and characterized a Mark **II** version of this kind of two-station rotaxane comprised of six molecular modules, namely (a) a bisparaphenylene[34]crown-10 electron donor macrocycle **M** and its dumbbell-shaped component which contains (b) a Ru(II)-polypyridine photoactive unit **P**²⁺ as one of its stoppers, (c) a *p*-terphenyl-type ring system as a rigid spacer **S**, (d) 4,4'-bipyridinium (**A**₁²⁺) and (e) 3,3'-dimethyl-4,4'-bipyridinium (**A**₂²⁺) electron acceptor units that can play the role of stations for the macrocycle **M**, and (f) a tetraarylmethane group **T** as the second stopper. This Mark **II** version is identical with **BR-I**⁶⁺ in the Mark **I** series that works as a sunlight-powered nanomotor (Balzani et al., *Proc. Natl. Acad. Sci. USA* **2006**, *103*, 1178), except for the swapping of the two stations **A**₁²⁺ and **A**₂²⁺ along the dumbbell-shaped component, i.e. the Mark **I** and **II** bistable rotaxanes are constitutionally isomeric. We have found the closer the juxtaposition of the electron transfer photosensitizer **P**²⁺ to the better (**A**₁²⁺) of the two electron acceptors, namely the situation in **BR-II**⁶⁺ compared with that in **BR-I**⁶⁺ results in an increase in the rate — and hence the efficiency — of the photoinduced electron-transfer step. The rate of the back electron transfer, however, also increases. As a consequence, **BR-II**⁶⁺ performs better than **BR-I**⁶⁺ in the fuel-assisted system, but much worse when it is powered by visible light (e.g. sunlight) alone. By contrast, when shuttling is electrochemically driven, the only difference between the two bistable rotaxanes in the Mark **I** and Mark **II** series is that the macrocycle **M** moves in opposite directions.

Manuscript received: 15 January 2006.

Final version: 23 February 2006.

Introduction

In the past few years synthetic prowess, which has always been the most distinguishing feature of chemists alongside other scientists, and device-driven ingenuity, which has evolved from chemists' preoccupation with reactivity, mechanism, and function, have led to the construction of a variety of molecular-level devices and machines.^[1–6] Much of the inspiration for the burgeoning of this field of functional molecular nanotechnology comes from the remarkable progress in molecular biology which has begun of late to reveal the secrets of the natural molecular-level devices and machines that constitute the material base of life.^[7,8] Despite some outstanding achievements,^[9–12] however, the bottom-up de novo construction of artificial devices and machines, as complex

as those present in nature, is a prohibitive task at this time. Hence, chemists have turned their attention to the construction of much simpler systems based on bi- and multi-stable catenanes and rotaxanes^[13–23] in which the relative mechanical movements of their components, caused by chemical, electrochemical, and photochemical inputs, can be detected and controlled.

In recent times, we have examined^[24,25] exhaustively the electrochemical and photophysical properties of a bistable rotaxane **BR-I**⁶⁺ composed of six molecular components — namely a bisparaphenylene[34]crown-10 (BPP34C10) electron-donating macrocycle **M** and a dumbbell-shaped component which contains (a) a Ru(II)-polypyridine photoactive unit **P**²⁺ as one of its stoppers,

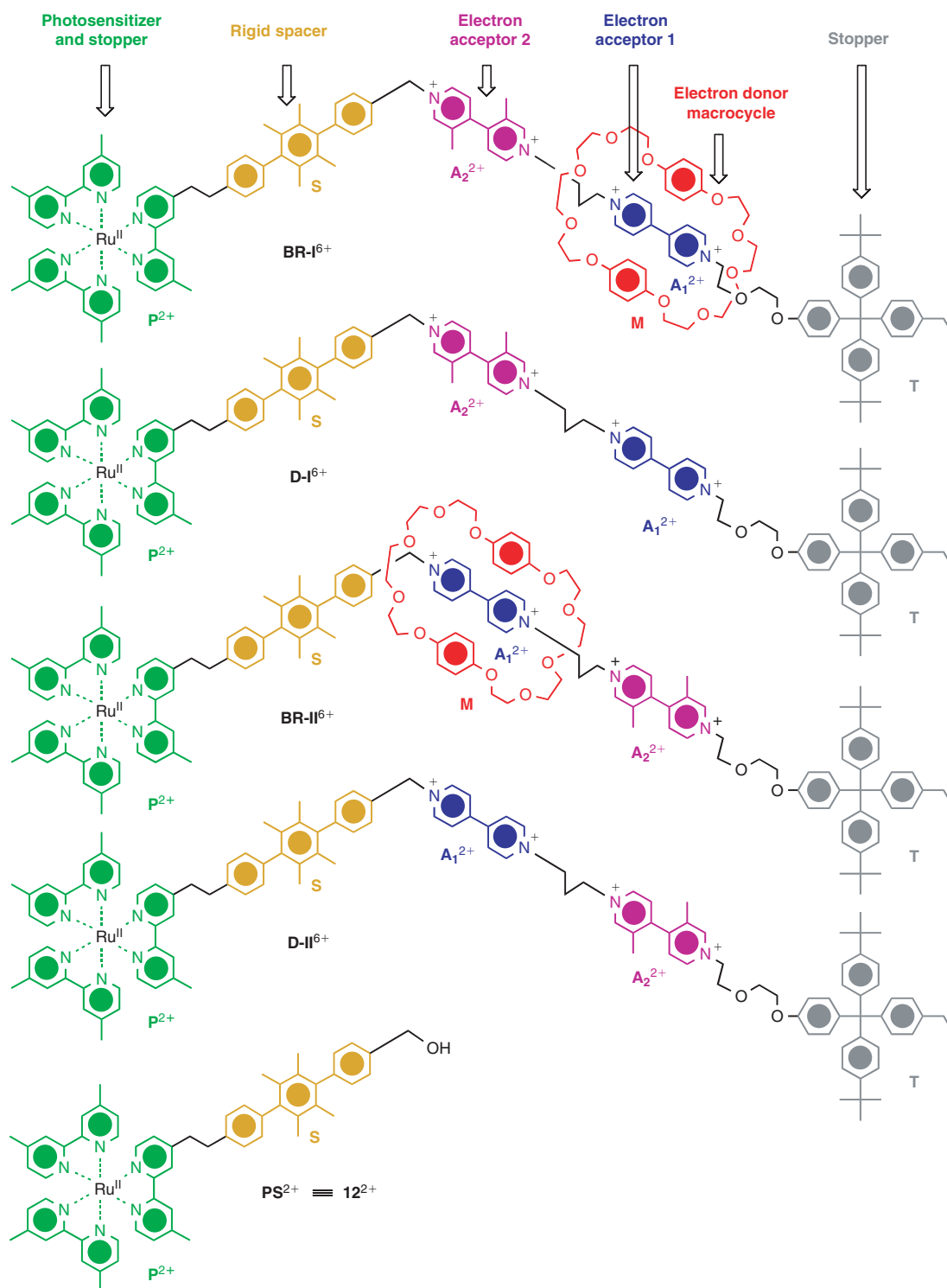
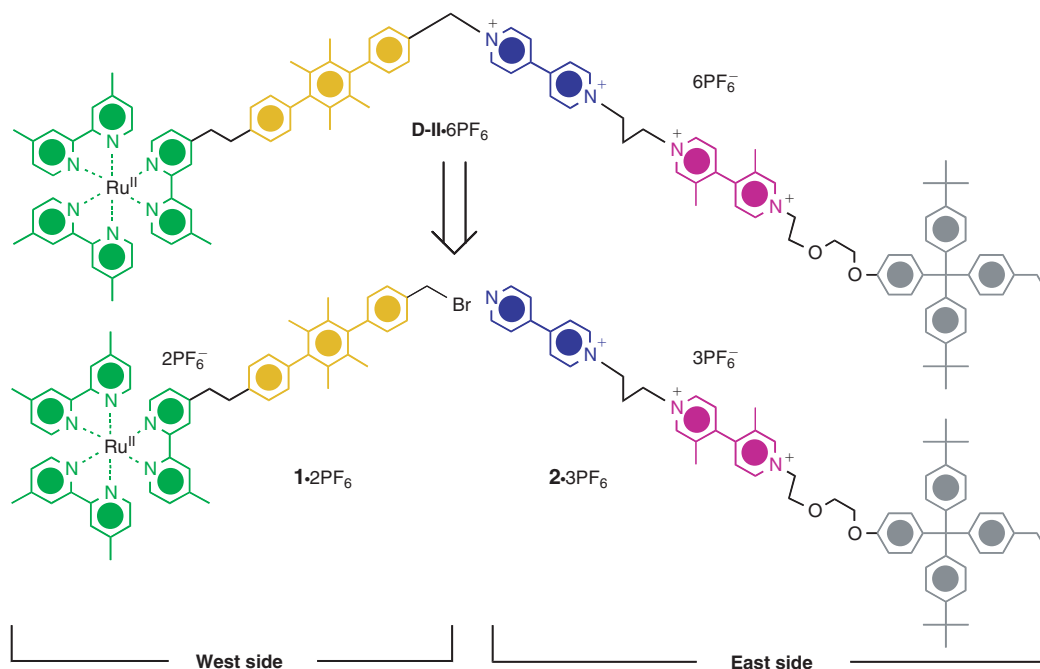


Fig. 1. Structural formulas of the rotaxanes **BR-I**⁶⁺ and **BR-II**⁶⁺, the corresponding dumbbell-shaped precursors **D-I**⁶⁺ and **D-II**⁶⁺, and the model photosensitizing compound **PS**²⁺ which have been investigated in this comparative study.

(b) a *p*-terphenyl-type ring system as a rigid spacer **S**, and (c) 4,4'-bipyridinium (**A**₁²⁺) and 3,3'-dimethyl-4,4'-bipyridinium (**A**₂²⁺) units as two electron-accepting units, that play the role of recognition sites or 'stations' for the macrocycle **M**, and (d) a tetraarylmethane group **T** as the second stopper. This Mark **I** version of a photochemically driven molecular-level abacus behaves^[25] as an autonomous

linear nanomotor and operates with quantum efficiency of about 12%.

We became intrigued to find out what would be the consequences for this autonomous artificial nanomotor powered by sunlight if we were to swap the two stations in the dumbbell-shaped component and produce a Mark **II** version, namely **BR-II**⁶⁺ which is essentially a constitutional isomer of the



Scheme 1. Retrosynthetic analysis for the synthesis of the dumbbell-shaped compound **D-II**·6PF₆, which is formed by a covalent attachment of two reactive intermediates — namely the ‘west side’ **1**·2PF₆ and the ‘east side’ **2**·3PF₆.

Mark **I** version. And so now, the Mark **II** version **BR-II**⁶⁺ (Fig. 1) has been synthesized and characterized. Our mission in this full paper is to compare the electrochemical and photochemical (under steady-state and pulsed irradiation) properties of these two versions (Mark **I** and **II**) in order to gain a better understanding of the role played by the various factors that determine the performance of this kind of molecular machine.

Results and Discussions

In order to have a set of data that is as meaningful as possible, we have investigated the properties of both of the bistable rotaxane **BR-II**⁶⁺ and its dumbbell-shaped precursor **D-II**⁶⁺, and we have compared the results obtained in this Mark **II** series with those previously reported^[24,25] in the Mark **I** series for rotaxane **BR-I**⁶⁺, its dumbbell-shaped precursor **D-I**⁶⁺, and compound **PS**²⁺ as a model for the photosensitizer **P**²⁺. The structural formulas of all these compounds are displayed in Fig. 1.

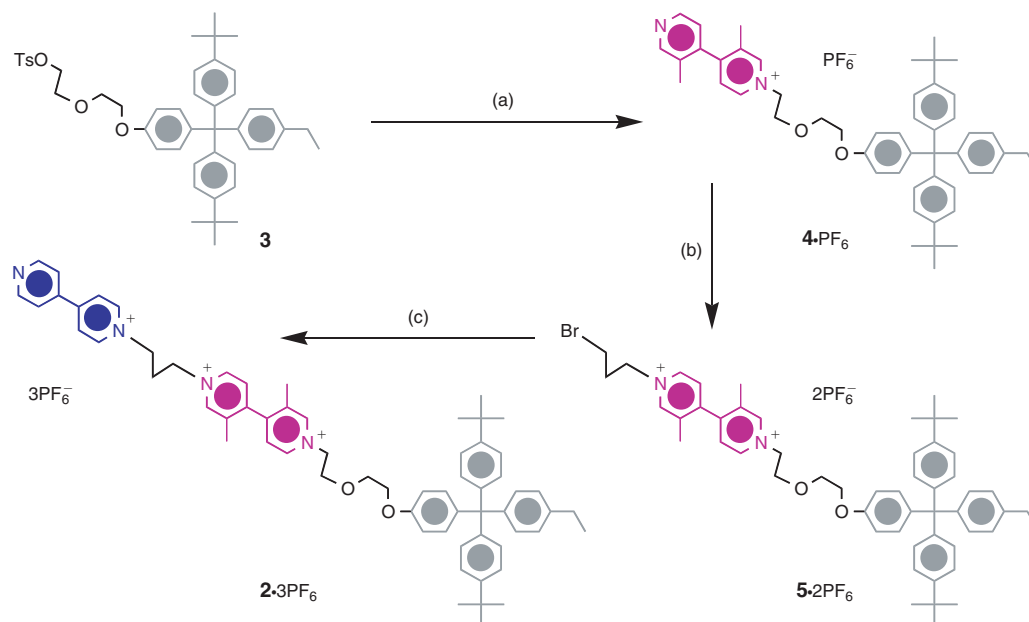
Synthesis and Structural Characterization

Based on our considerable experience^[24,25] gained during the preparation of the photochemically driven molecular-level abacus in the Mark **I** series, we have designed a bistable [2]rotaxane **BR-II**·6PF₆, comprising (a) a [Ru(bpy)₃]²⁺ type complex to act as the light-harvesting entity, that also serves as a stopper, (b) a 4,4'-bipyridinium unit and its 3,3'-dimethyl derivative to be the two π -electron accepting units, (c) a BPP34C10 macrocycle to serve as the π -electron donating ring component, (d) a *p*-terphenylene-type rigid spacer to separate the photoactive unit from the mechanical switching elements, and (e) a tetraarylmethane unit to act as a second

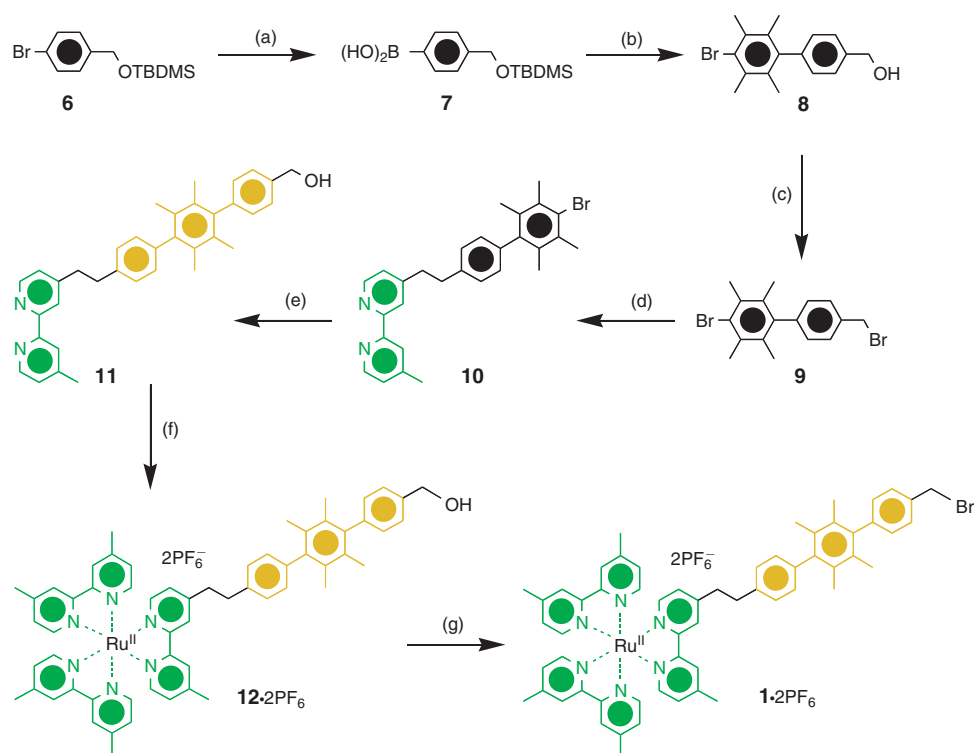
stopper at the other end of the abacus from the Ru(II) complex. The photoactive bistable rotaxane **BR-II**·6PF₆, and the corresponding dumbbell-shaped precursor **D-II**·6PF₆, were constructed in a modular fashion, starting with the syntheses of the active components and completing the sequence of events by bringing them together to make the target compounds. In order to simplify the synthetic route, the dumbbell-shaped precursor **D-II**·6PF₆ was dissected into two halves — as illustrated in the retrosynthetic analysis shown in Scheme 1 — the ‘west side’ **1**·2PF₆, which constitutes^[24] a light-harvesting moiety, composed of a [Ru(bpy)₃]²⁺ complex, tethered to a rigid *p*-terphenylene-type spacer containing a reactive benzyl bromide functionality, whereas the ‘east side’ **2**·3PF₆ constitutes^[24] the mechanical shuttling moiety containing a tetraarylmethane stopper adjacent to a 3,3'-dimethyl-4,4'-bipyridinium linked to a 4,4'-bipyridinium unit by means of a tris(methylene) spacer. In the first instance, the ‘east side’ containing two π -electron deficient recognition units and the ‘west side’ containing the Ru(II)-complex were synthesized separately. The linking of these two sides covalently afforded the dumbbell-shaped compound **D-II**·6PF₆. Slippage^[26] of the π -donating macrocycle BPP34C10 onto the **D-II**⁶⁺ yielded the bistable [2]rotaxane **BR-II**·6PF₆.

Constructing the ‘East Side’

The synthesis of the compound **2**·3PF₆ — the ‘east side’ — is outlined in Scheme 2. Treatment of the tosylate **3**^[24,29] with an excess amount of 3,3'-dimethyl-4,4'-bipyridine in refluxing MeCN in the presence of anhydrous LiBr afforded the monoquaternary salt **4**·PF₆, following counterion exchange (NH₄PF₆/H₂O/Me₂CO), in 81% yield. Alkylation of this compound with an excess of 1,3-dibromopropane, after counterion exchange (NH₄PF₆/H₂O), provided the diquaternary



Scheme 2. Synthesis of $2 \cdot 3PF_6$. Reagents and conditions: (a) (1) 3,3'-dimethyl-4,4'-bipyridine/LiBr/MeCN, reflux, 3 days; (2) $NH_4PF_6/H_2O/Me_2CO$, RT, 12 h. (b) (1) 1,3-dibromopropane/MeCN, reflux, 4 days; (2) $NH_4PF_6/H_2O/Me_2CO$, RT, 12 h. (c) (1) 4,4'-bipyridine/LiBr/MeCN, reflux, 7 days; (2) NH_4PF_6/H_2O , RT, 12 h.

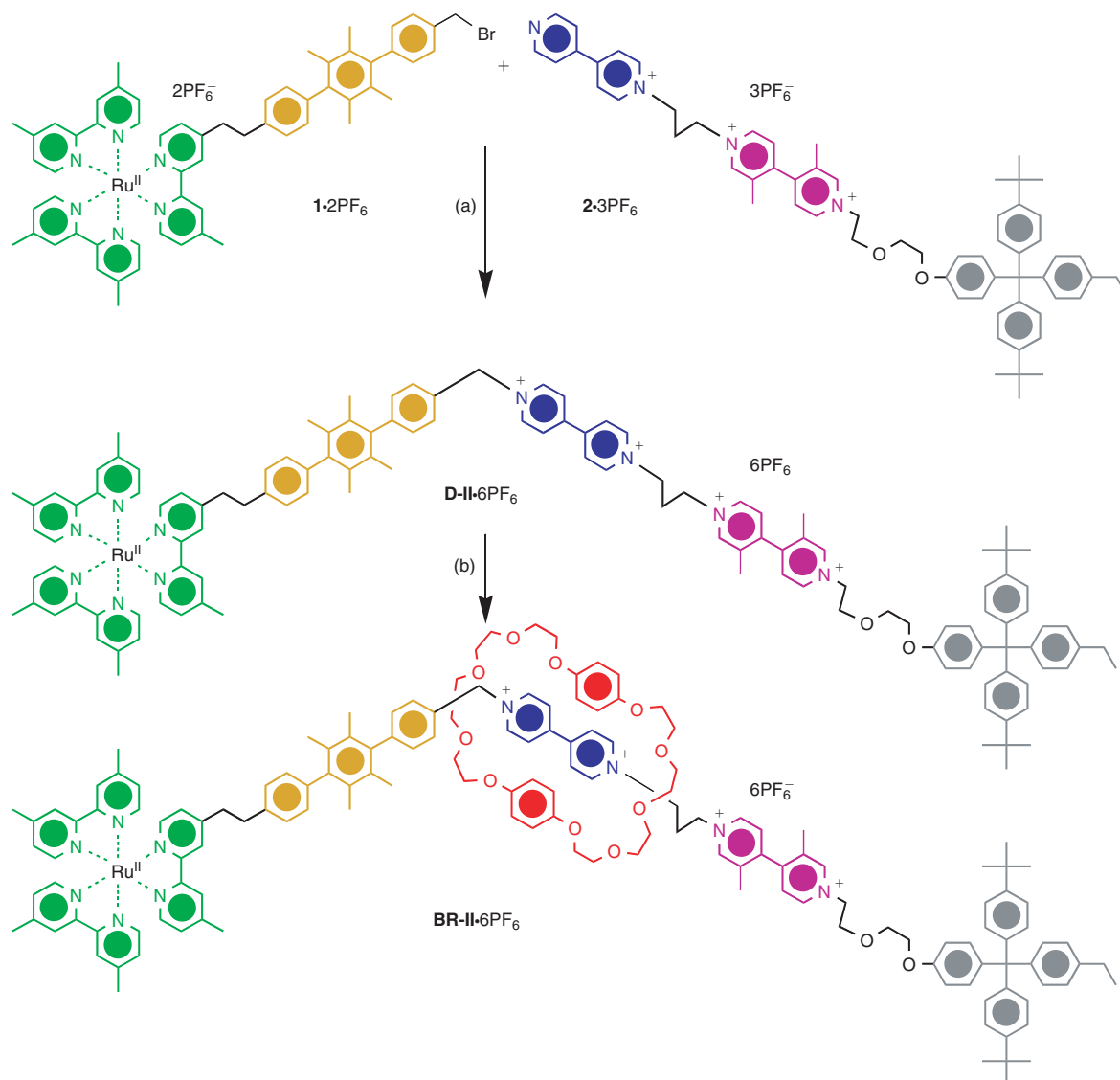


Scheme 3. Synthesis of $1 \cdot 2PF_6$. Reagents and conditions: (a) (1) Bu^uLi/THF , $-78^\circ C$, 1 h; (2) $B(OMe)_3$, $-78^\circ C$ to RT, 16 h; (3) 5% HCl, 30 min. (b) (1) 1,4-dibromo-2,3,5,6-tetramethylbenzene/ $2 M Na_2CO_3/Pd(PPh_3)_4/PhMe/EtOH$, reflux, 3 days; (2) TBAF/THF, RT, 12 h. (c) HBr/AcOH (45% w/v), reflux, 12 h. (d) dmbpy/LDA/THF, $-78^\circ C$ to RT, 12 h. (e) (1) 7/2 M $Na_2CO_3/Pd(PPh_3)_4/PhMe/EtOH$, reflux, 3 days; (2) TBAF/THF, RT, 12 h. (f) (1) $[Ru(4,4'-dmbpy)_2Cl_2]/EtOH/H_2O$, reflux, 24 h; (2) NH_4PF_6/H_2O , RT, 12 h. (g) (1) HBr/AcOH (45% w/v), reflux, 4 h; (2) NH_4PF_6/H_2O , RT, 12 h.

salt $5 \cdot 2PF_6$ in 55% yield. Reaction between $5 \cdot 2PF_6$ and 4,4'-bipyridine in MeCN under refluxing conditions generated, after counterion exchange (NH_4PF_6/H_2O), the trisquaternary salt $2 \cdot 3PF_6$ in 67% yield.

Constructing the 'West Side'

The synthesis of the ruthenium complex $1 \cdot 2PF_6$ — the 'west side' — is outlined in Scheme 3. The protected 4-bromobenzyl alcohol **6** was converted into the boronic acid



Scheme 4. Synthesis of **BR-II-6PF₆**. Reagents and conditions: (a) (1) MeCN, reflux, 6 days; (2) NH₄PF₆/H₂O, RT, 12 h. (b) BPP34C10/MeCN, 50°C, 4 days; (2) NH₄PF₆/H₂O, RT, 12 h.

derivative **7** in 79% yield by treatment with BuⁿLi, followed by trimethyl borate at -78°C. A Pd⁰-catalyzed cross coupling of the boronic acid **7** with 1,4-dibromo-2,3,5,6-tetramethylbenzene, followed by desilylation with tetrabutylammonium fluoride (TBAF), afforded the benzyl alcohol **8** in 75% overall yield. The alcohol **8** was then transformed into the benzyl bromide **9** in 89% yield by treatment with HBr in AcOH (45% w/v). Monolithiation of 4,4'-dimethyl-2,2'-bipyridine with equimolar amount of lithium diisopropylamide (LDA) in tetrahydrofuran (THF), followed by addition of the bromide **9**, generated the bipyridine derivative **10** in 66% yield. A Pd⁰-catalyzed cross coupling of the bromides **10** and **6**, followed by desilylation with TBAF, produced the benzyl alcohol **11** in 62% yield. The Ru(II) complex **12-2PF₆** was synthesized in 66% yield by exchanging a 4,4'-dimethyl-2,2'-bipyridine ligand from [Ru(4,4'-dimethyl-2,2'-bipyridine)₂]Cl₂ complex with **11** under refluxing conditions in a EtOH/H₂O mixture, followed by counterion exchange (NH₄PF₆/H₂O/Me₂CO).

The benzyl alcohol functionality was then converted to the corresponding benzyl bromide **1-2PF₆** in 90% yield by treating **12-2PF₆** with HBr in AcOH (45% w/v), followed by counterion exchange (NH₄PF₆/H₂O).

Attaching the 'East Side' to the 'West Side'

A mixture of **1-2PF₆** and **2-3PF₆** in MeCN was reacted under refluxing condition to obtain the dumbbell compound **D-II-6PF₆** in 57% yield, after counterion exchange (NH₄PF₆/H₂O), Scheme 4.

Generating the Bistable [2]Rotaxane by Slippage

Heating of the dumbbell compound **D-II-6PF₆** with six equivalents of BPP34C10 in MeCN at 50°C for 4 days afforded^[24] (Scheme 4) the bistable [2]rotaxane **BR-II-6PF₆**, after column chromatography (SiO₂: MeOH/2 M NH₄Cl/MeNO₂ 7/2/1) and counterion exchange (NH₄PF₆/H₂O), in 52% yield.

The rotaxane **BR-II**-6PF₆, its corresponding dumbbell **D-II**-6PF₆, and the intermediate components have all been characterized by ¹H and ¹³C NMR spectroscopy, absorption and luminescence spectroscopy, mass spectrometry, and elemental analyses, as well as by cyclic voltammetry.

Electrochemical Behavior

All electrochemical experiments were carried out in argon-purged MeCN solution at room temperature. Fig. 2 shows the cyclic voltammograms recorded for the bistable rotaxane **BR-II**⁶⁺ and its dumbbell-shaped precursor **D-II**⁶⁺. The results obtained are summarized in Table 1, where, for comparison purposes, the data relating to the bistable rotaxane **BR-I**⁶⁺, its dumbbell-shaped precursor **D-I**⁶⁺, the BPP34C10 macrocycle **M** and some model compounds of the two bipyridinium stations, are also displayed. The data recorded in Table 1 show that **BR-II**⁶⁺ and **D-II**⁶⁺ exhibit, respectively, ten and nine redox waves, that can be assigned in a straightforward manner. In particular, as far as the two electron-accepting stations are concerned, we should note the following. (a) For both **D-II**⁶⁺ and **D-I**⁶⁺, the first reduction potential can be assigned to the **A**₁²⁺ station and the second one to the **A**₂²⁺ one. (b) For both the Mark **I** and **II** variants, the first reduction wave is displaced to more negative values in going from the dumbbell to the bistable rotaxane; this behavior confirms that the stable translational isomer is the one in which the BPP34C10 macrocycle **M** encircles the **A**₁²⁺ station. (c) The second reduction wave is also displaced to more negative potentials in both variants on passing from the dumbbell to the bistable rotaxane; this result indicates that the BPP34C10 macrocycle **M** encircles the **A**₂²⁺ station after **A**₁²⁺ has been reduced to **A**₁⁺. (d) The small influence of the *p*-terphenyl unit in stabilizing the donor–acceptor interaction between BPP34C10 macrocycle **M** and the **A**₂²⁺ station, whose reduction shifts more to negative potentials in going from **BR-I**⁶⁺ to **BR-II**⁶⁺ compared with the corresponding dumbbell-shaped components, is evident.

In conclusion, the electrochemical results show that, in the ground state of the bistable rotaxane **BR-II**⁶⁺, the BPP34C10 macrocycle **M** encircles the **A**₁²⁺ station and that a one-electron reduction causes the deactivation of the **A**₁²⁺ station

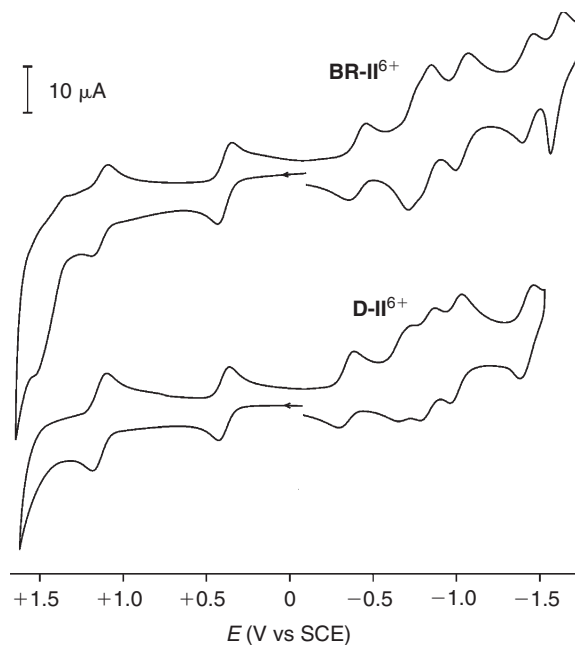


Fig. 2. Cyclic voltammograms (MeCN, room temperature, scan rate 200 mV s⁻¹) for **BR-II**⁶⁺ and **D-II**⁶⁺ in the potential range -1.5 and +1.6 V versus SCE.

with the consequent displacement of the BPP34C10 macrocycle **M** onto **A**₂²⁺. Reoxidation of **A**₁⁺ to **A**₁²⁺ allows the macrocycle **M** to return to the **A**₁²⁺ station. These results show that the electrochemically driven shuttling takes place in **BR-II**⁶⁺ exactly as it was reported^[24] previously for **BR-I**⁶⁺. The only difference between the two bistable rotaxanes is that the BPP34C10 macrocycle **M** moves in opposite directions, namely towards the sensitizer **P**²⁺ in **BR-I**⁶⁺ and towards the stopper **T** in **BR-II**⁶⁺.

Photochemical and Photophysical Behavior

It is well known that Ru(II) complexes of polypyridine ligands exhibit^[27] outstanding excited state and redox properties and that their photoinduced electron-transfer processes with bipyridinium-type compounds are fully reversible.^[28] We have shown^[24] previously that excitation with visible light

Table 1. Electrochemical data^A

Compound	Stopper	Crown ether	Ru	Viologen unit(s)				bpy ligands		
BR-II ⁶⁺	+1.64 ^B	+1.41 ^{C,D}	+1.13	-0.43	-0.77	-0.83	-1.04	-1.44	-1.6 ^E	-1.9 ^E
D-II ⁶⁺	+1.60 ^B		+1.14	-0.35	-0.69	-0.83	-1.00	-1.44	-1.6 ^E	-2.0 ^E
BR-I ⁶⁺	+1.70 ^B	+1.38 ^{C,D}	+1.14	-0.44	-0.73	-0.83	-1.00	-1.43	-1.62	^E
D-I ⁶⁺	+1.60 ^B		+1.15	-0.36	-0.68	-0.83	-0.96	-1.43	-1.59	^E
BPP34C10		+1.23 ^C +1.36 ^C								
PS ²⁺			+1.15					-1.43	-1.63	-1.87
1,1'-Dibenzyl-4,4'-bipyridinium dication				-0.36		-0.78				
1,1'-Dibenzyl-3,3'-dimethyl-4,4'-bipyridinium dication					-0.74		-0.94			

^AHalfwave potential values, V versus SCE; reversible and mono-electronic processes unless otherwise noted; see Experimental for details.

^BIrreversible process; potential value estimated from DPV peaks. ^CPoorly reversible process; potential value estimated from DPV peaks.

^DTwo-electron process. ^EThe observation of this process is hampered by adsorption phenomena.

of the bistable rotaxane **BR-I**⁶⁺ and the dumbbell precursor **D-I**⁶⁺ does indeed cause an electron transfer from the **P**²⁺ stopper to the **A**₁²⁺ station. It transpires that this mechanism also operates in the case of both the bistable rotaxane **BR-II**⁶⁺ and the dumbbell precursor **D-II**⁶⁺. Also, in both cases, the photoinduced electron transfer is followed by back electron transfer.

The spectroscopic and photophysical data obtained for **BR-II**⁶⁺ and **D-II**⁶⁺ are collected in Table 2 where the data reported^[24,25] previously for rotaxane **BR-I**⁶⁺, **D-I**⁶⁺, and the model compound **PS**²⁺ are also shown for comparison purposes. The absorption spectra of **BR-II**⁶⁺ (Fig. 3) and **D-II**⁶⁺ are commensurate with what would be predicted on the basis of the contributions from their chromophoric units. It should be noted that the weak charge transfer band (λ_{max} ca. 450 nm, ϵ_{max} ca. 500 L mol⁻¹ cm⁻¹)^[29] arising from the interaction between **A**₁²⁺ and **M** cannot be observed because it is hidden by the much more intense metal-to-ligand charge transfer (MLCT) band^[27] ($\lambda_{\text{max}} = 458$ nm with ϵ_{max} ca. 13400 L mol⁻¹ cm⁻¹ for **3**²⁺) associated with the ruthenium-based component **P**²⁺. Upon excitation at 450 nm, both **BR-II**⁶⁺ (Fig. 3) and **D-II**⁶⁺ exhibit the well known emission band^[24] with $\lambda_{\text{max}} = 618$ nm of component **P**²⁺. Both the lifetime and emission intensity are quenched (Table 2) when compared with the values found for the model compound **PS**²⁺. Under the experimental conditions employed (5×10^{-6} to 10^{-4} mol L⁻¹ solutions), the occurrence of dynamic quenching can be ruled out since the luminescence lifetime does not show any concentration dependence. The quenching constants k_{et} and yields of the electron transfer quenching process, Φ_{et} , have then been obtained (Table 3) from Eqns (1) and (2), where τ_0 is the luminescence lifetime of the reference compound **PS**²⁺

$$k_{\text{et}} = 1/\tau - 1/\tau_0 \quad (1)$$

$$\Phi_{\text{et}} = k_{\text{et}}\tau \quad (2)$$

No quenching is observed in a rigid matrix at 77 K, as expected for a moderately exoergonic electron transfer process because of the much larger solvent reorganizational energy. Comparison with the data reported^[24,25] previously shows that the quenching of the luminescent excited state of component **P**²⁺ is much more efficient for **BR-II**⁶⁺ and **D-II**⁶⁺ than it is for **BR-I**⁶⁺ and **D-I**⁶⁺. This observation means that the swapping of the positions of the two stations **A**₁²⁺ and **A**₂²⁺ along the dumbbell-shaped component increases

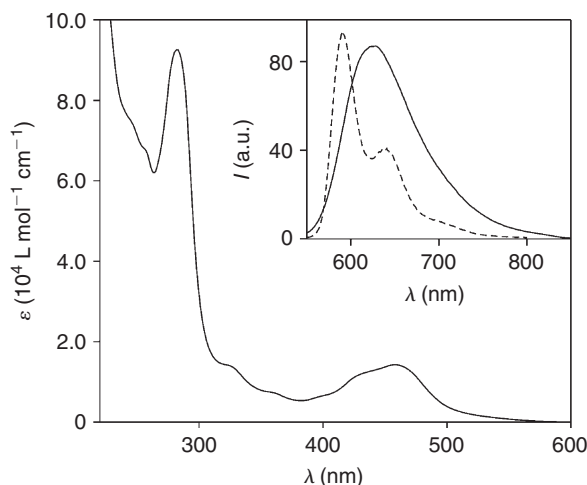


Fig. 3. Absorption and (inset) luminescence (MeCN, room temperature, full line; butyronitrile rigid matrix, 77 K, dashed line) spectra of a solution of **BR-II**⁶⁺. Excitation was performed at 450 nm.

the rate of the quenching process and therefore the efficiency of the forward electron transfer. This effect can hardly be attributed to the very small increase in the exoergonicity of the electron transfer process — in both the **BR**⁶⁺ compounds, the **A**₁²⁺ station is reduced at a potential 0.01 V less negative than in the **D**⁶⁺ compounds (Table 1). It seems more likely that the increase in the electron transfer rate is related to the decrease in the distance between **P**²⁺ and **A**₁²⁺, that, in **BR-II**⁶⁺ and **D-II**⁶⁺, is about 1 nm shorter than in **BR-I**⁶⁺ and **D-I**⁶⁺. It should also be noted that for the dumbbell-shaped compound the electron transfer efficiency increases by a factor of 1.5, whereas for the bistable rotaxane it increases by a factor of approximately 4. This behavior suggests that the BPP34C10 electron-donating macrocycle **M** that surrounds **A**₁²⁺ favors the electronic interaction between **P**²⁺ and **A**₁²⁺.

Continuous Irradiation in the Presence of Triethanolamine

It is well known^[30–32] that the photoreduction of bipyridinium ions (**Q**²⁺) by light excitation of ruthenium polypyridine compounds (e.g. [Ru(bpy)₃]²⁺, Eqn 3) is followed by a very fast back electron-transfer reaction (Eqn 4). As a consequence, transient formation of the **Q**⁺ species can only be observed in flash photolysis experiments. However, when the photoreaction is carried out in the presence of triethanolamine (TEOA), which is able to scavenge the oxidized [Ru(bpy)₃]³⁺-type species (Eqn 5) without appreciable

Table 2. Absorption and luminescence data^A

Compound	Absorption		Luminescence ^B			Luminescence 77 K ^{B,C}	
	λ_{max} [nm]	ϵ [L mol ⁻¹ cm ⁻¹]	λ_{max} [nm]	Φ	τ [ns]	λ_{max} [nm]	τ [μ s]
BR-II ⁶⁺	458	14200	620	0.028	440	591	4.8
D-II ⁶⁺	458	14500	620	0.042	640	591	4.6
BR-I ⁶⁺	458	14800	618	0.057	770	592	5.0
D-I ⁶⁺	458	15300	618	0.053	730	592	5.0
PS ²⁺	458	13400	618	0.065	880	592	5.0

^AData obtained in degassed MeCN solution at room temperature, unless otherwise noted. ^BExcitation at 450 nm. ^CButyronitrile rigid matrix.

Table 3. Electron transfer data^A

Compound	k_{et} [s^{-1}]	Φ_{et}	τ_{bet} [μs]	k_{bet} [s^{-1}]
BR-II ⁶⁺	1.1×10^6	0.50	<0.2	$>5 \times 10^6$
D-II ⁶⁺	4.3×10^5	0.27	<0.2	$>5 \times 10^6$
BR-I ⁶⁺	1.6×10^5	0.13	7.1 ^B	1.4×10^5 ^B
D-I ⁶⁺	2.3×10^5	0.18	1.4 ^B	7.0×10^5 ^B

^ASubscripts: et: forward electron transfer (Fig. 5, step 2). bet: back electron transfer (Fig. 5, steps 5 and 6). ^BObtained by nanosecond laser flash photolysis experiments at 299 K, see ref. [25].

quenching of the $[\text{Ru}(\text{bpy})_3]^{2+}$ -type excited states, the reduced Q^+ species can accumulate



When photoexcitation of **BR-II**⁶⁺ or **D-II**⁶⁺ (ca. $5 \times 10^{-5} \text{ mol L}^{-1}$) was performed with a continuous 436-nm light in a degassed MeCN solution containing 0.05 mol L^{-1} TEOA, strong spectral changes (see e.g. Fig. 4) were observed. Comparison with the known spectra of model compounds^[24] shows clearly that the photochemical reaction causes a permanent reduction of A_1^{2+} to A_1^+ . After 30 min of irradiation, 100% of the A_1^{2+} units were monoreduced. Continuing irradiation for 30 additional minutes did not cause any further spectral change, showing that the A_1^+ species are stable and that the A_2^{2+} units are not reduced under the experimental conditions used — the spectrum^[33] of A_2^+ is substantially different from that^[34] of A_1^+ . If dioxygen was allowed to enter the irradiated solution, the complete disappearance of the characteristic bands of A_1^+ was observed, with recovery of the original spectroscopic properties of

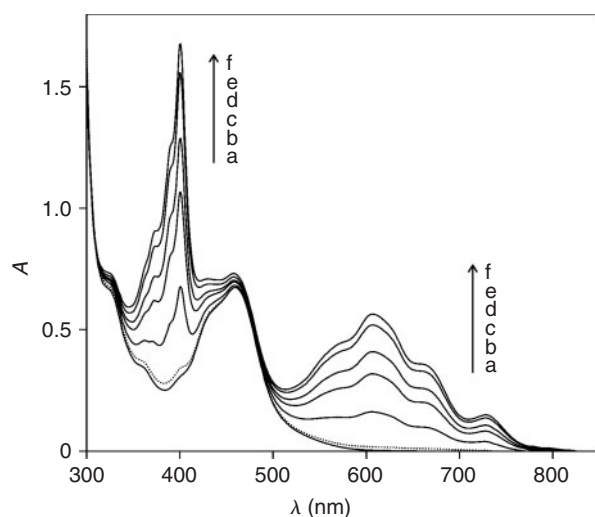


Fig. 4. Spectral changes observed upon photoexcitation of **BR-II**⁶⁺ ($4.7 \times 10^{-5} \text{ mol L}^{-1}$) with 436-nm light in the presence of 0.05 mol L^{-1} triethanolamine in a degassed MeCN solution at room temperature. Irradiation times are (a)–(f) 0, 1, 3, 5, 10, and 30 min. Prolonging irradiation for 30 more minutes did not cause further spectral changes. Upon exposure of the irradiated solution to air for 2 min, the absorption spectrum represented with a dotted line was obtained. Similar spectral changes were observed in the case of **D-II**⁶⁺.

BR-II⁶⁺ or **D-II**⁶⁺. Exactly the same behavior was observed^[24] previously for **BR-I**⁶⁺ and **D-I**⁶⁺.

Flash Photolysis Experiments

We have reported^[24,25] previously that, in the case of model compound **PS**²⁺, where photoinduced electron transfer cannot take place because it does not contain any electron acceptor unit, the observed spectral changes were consistent with the formation of the excited state of the P^{2+} unit. An isosbestic point between the absorption spectra of the ground and excited states of the P^{2+} unit in this model compound was found at $\lambda_{\text{iso}} = 398 \text{ nm}$ and was then used to measure the electron transfer rate constants (see below). Upon flash excitation of **BR-I**⁶⁺ in deaerated MeCN solutions, transient absorption spectral changes were also observed.^[25] The transient spectrum recorded $6 \mu\text{s}$ after light excitation displayed the features of the monoreduced 4,4'-bipyridinium unit A_1^+ , and some residual bleaching in the spectral region of the ground state absorption of P^{2+} . There was no evidence for the formation of the monoreduced 3,3'-dimethyl-4,4'-bipyridinium unit, A_2^+ . The same results were obtained for **D-I**⁶⁺. For both **BR-I**⁶⁺ and **D-I**⁶⁺, the formation and decay of the A_1^+ unit was monitored at $\lambda_{\text{iso}} = 398 \text{ nm}$ and the rate constants for the forward ($*\text{P}^{2+}$ to A_1^{2+}) and the back (A_1^+ to P^{3+}) were measured (Table 3) at five different temperatures. The quantum yields of the photoinduced electron transfer processes obtained from transient absorption data were in agreement, within experimental error, with those found from luminescence measurements.

When the same experiments were performed on **BR-II**⁶⁺ and **D-II**⁶⁺, the results obtained were quite different. For both compounds there was no spectral change at $\lambda_{\text{iso}} = 398 \text{ nm}$. Since we know from the experiments performed in the presence of TEOA that the quenching of the $*\text{P}^{2+}$ excited state by A_1^{2+} in **BR-II**⁶⁺ and **D-II**⁶⁺ is indeed caused by an electron transfer process with formation of A_1^+ (see above), we must conclude that A_1^+ cannot accumulate unless the oxidized P^{3+} species is rapidly scavenged. This observation means that, for **BR-II**⁶⁺ and **D-II**⁶⁺, the rate of the back electron transfer from A_1^+ to P^{3+} is faster than the forward reactions, and so is contrary to what happens^[25] in the case of **BR-I**⁶⁺ and **D-I**⁶⁺.

In the previous paper^[25] we used phenothiazine as electron relay. With the present **BR-II**⁶⁺ shuttle we could not do that because, in order to compete with the very fast back electron transfer process, a too high concentration of phenothiazine should have been used. Under such conditions direct reductive quenching of the $*\text{P}^{2+}$ excited state^[35] would have prevented the forward electron transfer.

Shuttling of the Macrocycle

The bistable rotaxane **BR-I**⁶⁺ was synthesized with the aim^[24,25] of obtaining an autonomous nanomotor powered solely by visible light. Subsequently, we synthesized **BR-II**⁶⁺ to gain a better understanding of the role played by the structure of the dumbbell with the purpose of optimizing the performance of these sunlight-powered nanomotors. The suggested mechanism, illustrated in the left part of Fig. 5

for **BR-II**⁶⁺, is based on the following four phases (see also Fig. 6)

(a) *Destabilization of the stable co-conformation*: Light excitation of the photoactive unit **P**²⁺ (step 1) is followed by the transfer of an electron from the ***P**²⁺ excited state to the **A**₁²⁺ station, which is encircled by the macrocycle

M (step 2), with the consequent ‘deactivation’ of this station; such a photoinduced electron-transfer process has to compete with the intrinsic decay of ***P**²⁺ (step 3).

(b) *Macrocycle displacement*: After reduction (‘deactivation’) of the **A**₁²⁺ station to **A**₁⁺, the macrocycle moves by Brownian motion to **A**₂²⁺ (step 4), a step that has

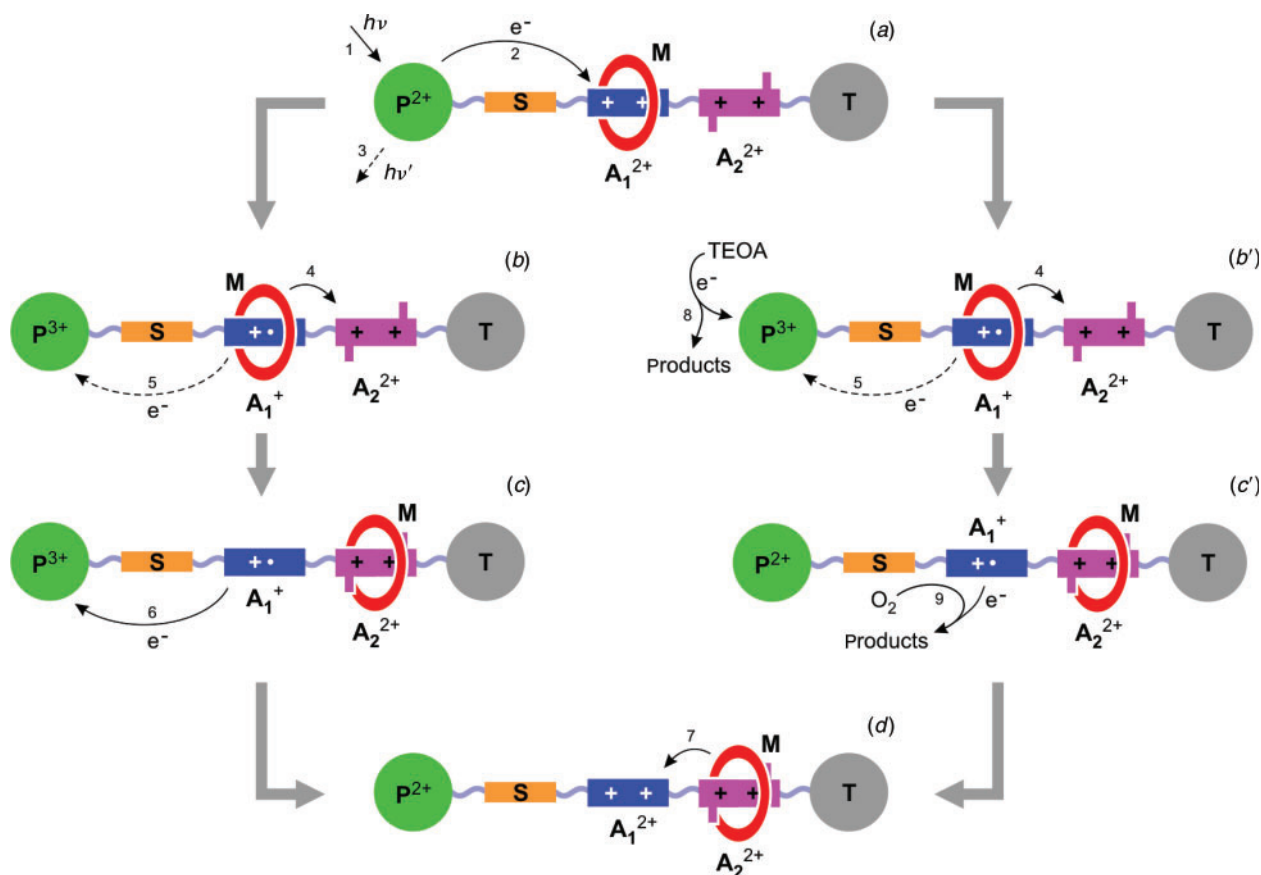


Fig. 5. Mechanisms of the photochemically driven ring shuttling in **BR-II**⁶⁺. Left, intramolecular mechanism. Right, mechanism assisted by two low-energy fuels, namely triethanolamine (TEOA) and dioxygen. For more details, refer to the text.

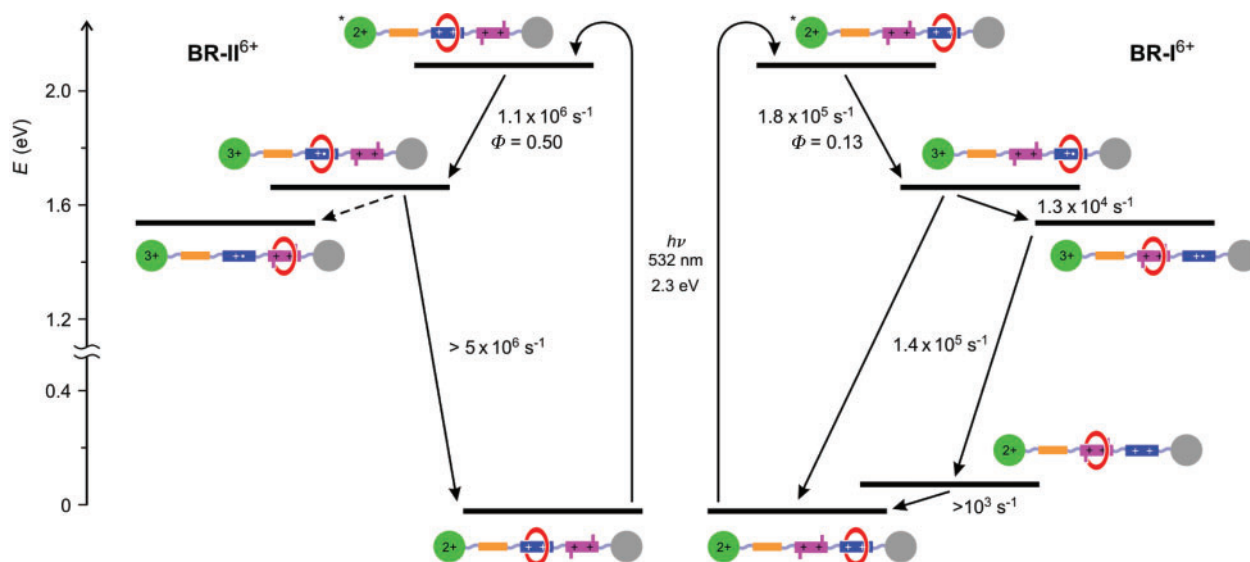


Fig. 6. Schematic energy level diagrams for the processes taking place in **BR-II**⁶⁺ (left-hand side) and **BR-I**⁶⁺ (right-hand side) after excitation with visible light. The process indicated with a dashed arrow for **BR-II**⁶⁺ does not occur in practice. For more details, refer to the text.

to compete with back electron-transfer from \mathbf{A}_1^+ to the oxidized photoactive unit \mathbf{P}^{3+} (step 5).

- (c) *Electronic reset*: A back electron-transfer process from the 'free' reduced station \mathbf{A}_1^+ to \mathbf{P}^{3+} (step 6) restores the electron acceptor power of the \mathbf{A}_1^{2+} station.
- (d) *Nuclear reset*: As a consequence of the electronic reset, the macrocycle \mathbf{M} moves back again by Brownian motion from \mathbf{A}_2^{2+} to \mathbf{A}_1^{2+} (step 7).

The quantum yield of the shuttling process (Φ_{sh} , number of shuttling events divided by number of absorbed photons) is given by Eqn (6)

$$\Phi_{\text{sh}} = \Phi_{\text{et}} \times \eta_{\text{rd}} \times \eta_{\text{er}} \times \eta_{\text{nr}} \quad (6)$$

where Φ_{et} is the quantum yield of the photoinduced electron transfer process that causes the destabilization of the initial co-conformation, η_{rd} the efficiency of ring displacement, η_{er} the efficiency of the electronic reset, and η_{nr} the efficiency of the nuclear reset. Since the efficiency of the nuclear reset, η_{nr} , is equal to 1 (k_7 does not compete with any other step), Eqn (6) reduces to

$$\Phi_{\text{sh}} = \Phi_{\text{et}} \times \eta_{\text{rd}} \times \eta_{\text{er}} \quad (7)$$

In this paper, we have demonstrated that shuttling of the macrocycle \mathbf{M} can be achieved easily by alternate electrochemical reduction/reoxidation of \mathbf{A}_1^{2+} , as well as by a photochemical mechanism involving the assistance of two low energy fuels. In the latter case (right part of Fig. 5), after the photoinduced electron transfer process from $^*\mathbf{P}^{2+}$ to \mathbf{A}_1^{2+} , the sacrificial reductant TEOA donates irreversibly one electron to the oxidized \mathbf{P}^{3+} unit (step 8) before back electron transfer (step 5) can occur and, as the \mathbf{A}_1^+ unit is formed, the macrocycle \mathbf{M} moves to \mathbf{A}_2^{2+} (step 4). Upon addition of a sacrificial oxidant (e.g. O_2) to the solution, the \mathbf{A}_1^+ unit is back oxidized to \mathbf{A}_1^{2+} (step 9) and the macrocycle moves back to the original position (step 7).

Under the experimental conditions used, the scavenging of \mathbf{P}^{3+} by TEOA and the back oxidation of \mathbf{A}_1^+ to \mathbf{A}_1^{2+} by dioxygen are 100% efficient, so that the efficiency of the shuttling process depends only on the competition between the transfer of an electron from the $^*\mathbf{P}^{2+}$ excited state to the \mathbf{A}_1^{2+} station and the intrinsic decay of $^*\mathbf{P}^{2+}$ (step 3), that is

$$\Phi_{\text{sh}} = \Phi_{\text{et}} \quad (8)$$

The data obtained (Table 3) show that such a fuel-assisted process is more efficient in the case of rotaxane **BR-II**⁶⁺ than it is in the case of **BR-I**⁶⁺. This result was indeed expected because the swapping of the two stations decreases the distance between the two reaction partners in the Mark **II** version.

The swapping of the two stations, however, increases, not only the rate of the forward, but also that of the back electron transfer process. Indeed we have found that, in the case of **BR-II**⁶⁺, no transient formation of \mathbf{A}_1^+ can be observed in flash photolysis experiments, indicating that the rate of the back-electron transfer reaction must be faster than that of the forward electron transfer process by about $5 \times 10^6 \text{ s}^{-1}$

(Fig. 6). Since the rate of the displacement of the macrocycle is very slow ($1.3 \times 10^4 \text{ s}^{-1}$ for **BR-I**⁶⁺ at 299 K),^[25] the macrocycle displacement efficiency η_{rd} , which is 0.09 for **BR-I**⁶⁺ at 299 K, is negligible for **BR-II**⁶⁺.

Conclusions

Whereas electrochemically there is nothing to choose between the behavior of the Mark **I** and **II** versions — namely the constitutional isomers **BR-I**⁶⁺ and **BR-II**⁶⁺, respectively — photochemically they behave quite differently. The closer the electron transfer photosensitizer \mathbf{P}^{2+} to the better electron acceptor \mathbf{A}_1^{2+} in the Mark **II** compared with the Mark **I** shuttle, the faster are the rates of both the photoinduced electron transfer and the back electron transfer steps. The consequence is that, while the Mark **II** version performs best when it is fuel-assisted, it is nothing like as efficient as the Mark **I** system when it is powered by visible light (sunlight) on its own. In the electrochemically driven situation, the only difference between the two bistable rotaxanes is that the macrocycle moves in opposite directions, i.e. towards the sensitizer \mathbf{P}^{2+} in the Mark **I** rotaxane and towards the stopper **T** in the Mark **II** rotaxane.

Experimental

Materials and Techniques

All reactions were carried out under N_2 atmospheres. Chemicals were purchased from Aldrich and used as received. 2-[4-[4-ethylphenyl-bis(4-*tert*-butylphenyl)methyl]phenoxy]ethoxyethanol 4-methyl benzenesulfonate^[24,29] (**3**), 3,3'-dimethyl-4,4'-bipyridine,^[36] 4-bromobenzyl *tert*-butyldimethylsilyl ether^[37] (**6**), 1,4-dibromo-2,3,5,6-tetramethylbenzene,^[38] $[\text{Ru}(4,4'\text{-dimethyl-2,2'\text{-bipyridine)}_2\text{Cl}_2 \cdot 2\text{H}_2\text{O})]$,^[39] and BPP34C10 were synthesized^[40] according to literature procedures. The 4,4'-dimethyl-2,2'-bipyridine, *tert*-butyldimethylsilyl, and *p*-toluenesulfonyl groups are identified by the abbreviations dmbpy, TBDMS, and Ts, respectively. Yields refer to chromatographically pure products. Thin-layer chromatography (TLC) was carried out on aluminum sheets coated with silica gel 60 (Merck 5554). Column chromatography was performed on silica gel 60 (Merck, 40–60 nm). Melting points were determined on an Electrothermal 9200 melting point apparatus. Microanalysis were performed by the University of Sheffield Microanalytical Laboratories or by the University of North London Microanalytical Services. Liquid secondary ion mass spectra (LSIMS) were recorded on a VG ZabSpec mass spectrometer equipped with a Cs ion source using *m*-nitrobenzyl alcohol containing a trace of NaOAc. For accurate mass measurements using high-resolution LSIMS (HRLSIMS), the instrument was operated at a resolution of ca. 6000 by narrow-range voltage scanning along with polyethylene glycol or CsI as reference compounds. Electrospray ionization mass spectra (ESIMS) were measured on a VG ProSpec triple focussing mass spectrometer using MeCN as mobile phase. Electron impact (EI) MS were recorded at 70 eV on a VG ProSpec mass spectrometer. ¹H and ¹³C NMR and spectra were recorded on either a Bruker AC300 or a Bruker AMX400 or a Bruker DRX500 spectrometer. The following abbreviations are used for the signal multiplicities or characteristics: s singlet, d doublet, dd double doublet, t triplet, m multiplet, q quartet, and br broad.

N-[2-[4-[4-Ethylphenyl-bis(4-*tert*-butylphenyl)methyl]phenoxy]ethoxy]ethyl] 3',3'-Di-methyl-4,4'-bipyridinium Hexafluorophosphate **4-PF₆**

A mixture of 2-[4-[4-ethylphenyl-bis(4-*tert*-butylphenyl)methyl]phenoxy]ethoxyethanol 4-methyl benzene-sulfonate^[24,29] (**3**) (1.64 g, 2.28 mmol), 3,3'-dimethyl-4,4'-bipyridine^[34] (2.34 g, 12.72 mmol), and anhydrous LiBr (70 mg) in dry MeCN (14 mL) was heated under reflux

for 3 days. The solvent was evaporated to dryness and the crude product was purified by column chromatography (SiO₂/the first eluent was MeOH to remove an excess of 3,3'-dimethyl-4,4'-bipyridine and the second eluent was MeOH/MeNO₂/2 M NH₄Cl 8/1.9/0.1). The isolated residue was dissolved in H₂O/Me₂CO and a saturated aqueous solution of NH₄PF₆ was added. After the evaporation of the Me₂CO, the precipitated solid was filtered off, washed with H₂O, and dried (70°C/0.1 Torr) to yield 4-PF₆ (1.62 g, 81%). δ_H (300 MHz, CD₃CN, 25°C) 1.18 (t, *J* 8 Hz, 3H), 1.27 (s, 18H), 2.03 (s, 3H), 2.08 (s, 3H), 2.58 (q, *J* 8 Hz, 2H), 3.79–3.83 (m, 2H), 3.99–4.07 (m, 4H), 4.68 (t, *J* 4.7 Hz, 2H), 6.76 (d, *J* 8.9 Hz, 2H), 7.09–7.14 (m, 10H), 7.27 (d, *J* 8.5 Hz, 4H), 7.69 (d, *J* 6.2 Hz, 2H), 8.60 (d, *J* 6.2 Hz, 1H), 8.67 (s, 1H).

N-[3-(3-Bromopropyl)-*N'*-[2-[4-[4-ethylphenyl-bis(4-tert-butylphenyl)methyl]phenoxy]ethoxy]-ethyl] 3',3'-Dimethyl-4,4'-bipyridinium Bis(hexafluorophosphate) 5-2PF₆

A solution of 4-PF₆ (1.01 g, 1.15 mmol) and 1,3-dibromopropane (2.32 g, 11.5 mmol) in dry MeCN (15 mL) was heated under reflux for 4 days. The solvent was removed under reduced pressure and the residue was purified by column chromatography (SiO₂: MeOH/MeNO₂/2 M NH₄Cl 8/1.9/0.1) to afford, after counterion exchange (H₂O/Me₂CO, a saturated aqueous solution of NH₄PF₆), 5-2PF₆ (720 mg, 55%) as a white-gray solid. δ_H (300 MHz, CD₃COCD₃, 25°C) 1.19 (t, *J* 8 Hz, 3H), 1.28 (s, 18H), 2.38 (s, 3H), 2.40 (s, 3H), 2.60 (q, *J* 7.5 Hz, 2H), 2.70–2.82 (m, 2H), 3.65 (t, *J* 6.5 Hz, 2H), 3.91 (t, *J* 4.3 Hz, 2H), 4.13 (t, *J* 4.3 Hz, 2H), 4.23 (t, *J* 4.6 Hz, 2H), 4.98–5.09 (m, 4H), 6.83 (d, *J* 8.8 Hz, 2H), 7.07–7.13 (m, 10H), 7.30 (d, *J* 8.5 Hz, 4H), 8.17 (d, *J* 6.2 Hz, 1H), 8.24 (d, *J* 6.2 Hz, 1H), 9.19 (t, *J* 6.8 Hz, 2H), 9.30 (d, *J* 7 Hz, 2H).

N-[3-(4,4'-bipyridinium-1-yl)propyl]-*N'*-[2-[4-[4-ethylphenyl-bis(4-tert-butylphenyl)methyl]-phenoxy]ethoxy]ethyl] 3',3'-Dimethyl-4,4'-bipyridinium Tris(hexafluorophosphate) 2-3PF₆

A solution of 5-2PF₆ (710 mg, 0.62 mmol) and 4,4'-bipyridine (970 mg, 6.2 mmol) in dry MeCN (14 mL) was heated under reflux for 7 days. After removal of the solvent, the residue was purified by column chromatography (SiO₂: MeOH/2 M NH₄Cl/MeNO₂ 7/2/1) to afford, after counterion exchange (50% aqueous solution of NH₄PF₆), 2-3PF₆ (570 mg, 67%) as a light brown solid. δ_H (300 MHz, CD₃CN, 25°C) 1.18 (t, *J* 8 Hz, 3H), 1.27 (s, 18H), 2.20 (s, 3H), 2.23 (s, 3H), 2.59 (q, *J* 7.5 Hz, 2H), 2.65–2.83 (m, 2H), 3.82 (t, *J* 4.3 Hz, 2H), 4.06–4.11 (m, 4H), 4.67–4.78 (m, 4H), 6.82 (d, *J* 8.8 Hz, 2H), 7.12–7.17 (m, 10H), 7.30 (d, *J* 8.6 Hz, 4H), 7.77–7.95 (m, 4H), 8.40 (d, *J* 6.8 Hz, 2H), 8.70 (d, *J* 6.2 Hz, 2H), 8.77 (br s, 2H), 8.85 (d, *J* 6.9 Hz, 4H).

4-(tert-Butyldimethylsilyloxymethyl)phenylboronic Acid 7

A solution of 4-bromobenzyl tert-butyldimethylsilyl ether^[37] (6) (12.0 g, 40 mmol) in anhydrous THF (80 mL) was cooled to –78°C under nitrogen atmosphere and a solution of BuⁿLi (1.6 M in hexanes, 27.5 mL, 44.0 mmol) was added slowly. After stirring the mixture at –78°C for 1 h, B(OMe)₃ (8.3 g, 80 mmol) was added slowly, while maintaining the temperature below –65°C and then stirring was continued for another 1 h at –78°C. The mixture was allowed to warm up to room temperature and stirred for additional 16 h. Hydrochloric acid (5%, 40 mL) was added to the ice-cooled stirred mixture which was then extracted several times with Et₂O. The combined organic layers were washed with water and brine, and dried over MgSO₄. Filtration and evaporation of the solvent gave the crude product, which was purified by column chromatography (SiO₂: hexanes/EtOAc 3/1) to yield the boronic acid 7 (8.4 g, 79%) as a white solid. mp 144°C. δ_H (300 MHz, CDCl₃, 25°C) 0.12 (s, 6H), 0.97 (s, 9H), 4.84 (s, 2H), 7.44, 7.47, 8.19, 8.22 ppm (AA'BB', 4H). δ_C (75.5 MHz, CDCl₃, 25°C) –5.2, 18.4, 26.0, 65.0, 125.5, 128.8, 135.7, 146.2. (Found: C 58.88, H 8.65. Calc. for C₁₃H₂₃BO₃Si: C 58.65, H 8.71%.)

4-(4-Bromo-2,3,5,6-tetramethylphenyl)benzyl Alcohol 8

An aqueous solution of Na₂CO₃ (2 M solution, 10 mL, 20 mmol) and the catalyst Pd(PPh₃)₄ (0.46 g, 5 mol%) were added to a solution of 1,4-dibromo-2,3,5,6-tetramethyl benzene^[38] (11 g, 37.6 mmol) in PhMe

(75 mL). After purging the mixture with N₂ for 15 min, the boronic acid 7 (2 g, 7.52 mmol), dissolved in EtOH (8 mL), was added. The reaction mixture was heated under reflux for 3 days, during which time it turned black. The mixture was cooled down to room temperature before being diluted with EtOAc (80 mL) and H₂O (80 mL). The aqueous layer was discarded and the organic layer was washed with H₂O, brine and dried (MgSO₄). Evaporation of solvent in vacuo gave a residue from which an excess of 1,4-dibromo-2,3,5,6-tetramethylbenzene was recovered by crystallization from MeOH. After removal of solvent from the mother liquor, the residue was subjected to desilylation by treating with TBAF (1 M solution in THF, 25 mL, 25 mmol) in THF (75 mL) at room temperature for 12 h. The solvent was removed under reduced pressure and the crude product was purified by column chromatography (SiO₂: CH₂Cl₂) to yield the alcohol 8 (1.8 g, 75%), as a white solid. mp 112°C. δ_H (300 MHz, CDCl₃, 25°C) 1.80 (s, 1H), 1.96 (s, 6H), 2.45 (s, 6H), 4.77 (s, 2H), 7.07, 7.09, 7.41, 7.44 ppm (AA'BB', 4H). δ_C (75.5 MHz, CDCl₃, 25°C) 19.2, 21.2, 65.3, 127.2, 128.4, 129.4, 133.5, 133.8, 139.2, 140.9, 141.6. (Found: C 64.08, H 6.12. Calc. for C₁₇H₁₉BrO: C 63.96, H 6.00%.)

4-(4-Bromo-2,3,5,6-tetramethylphenyl)benzyl Bromide 9

A solution of the alcohol 8 (2.3 g, 7.2 mmol) in 40 mL HBr/AcOH (45%, w/v) was heated under reflux for 12 h before being cooled down to room temperature and poured into ice-water (200 mL). The mixture was neutralized with 5% NaHCO₃ and extracted several times with CH₂Cl₂. The combined organic layers were washed with H₂O, brine and dried (MgSO₄). Removal of the solvent afforded the crude product, which was purified by column chromatography (SiO₂: hexanes/CH₂Cl₂ 100/4) to afford the bromide 9 (2.4 g, 89%) as a white solid. mp 116°C. δ_H (300 MHz, CDCl₃, 25°C) 1.95 (s, 6H), 2.45 (s, 6H), 4.56 (s, 2H), 7.05, 7.07, 7.43, 7.46 (AA'BB', 4H). δ_C (75.5 MHz, CDCl₃, 25°C) 19.1, 21.1, 33.4, 128.5, 129.2, 129.7, 133.3, 133.9, 136.2, 140.5, 142.4. *m/z* (EIMS, 70 eV) 382 (M⁺, 46), 338 (13), 301 (100), 223 (22), 207 (65), 192 (46), 178 (27). (Found: C 53.53, H 4.78. Calc. for C₁₇H₁₈Br₂: C 53.43, H 4.75%.)

4-[2-[4-[4-Bromo-2,3,5,6-tetramethylphenyl]phenyl]ethyl]-4'-methyl-2,2'-bipyridine 10

A solution of dmbpy (1.0 g, 5.43 mmol) in dry THF (45 mL) was added dropwise (15 min) at –78°C to a stirred solution of a freshly prepared lithium di-isopropyl amine (LDA) and BuⁿLi (1.6 M in hexane, 3.5 mL, 5.6 mmol) in dry THF (10 mL), which turned into a dark brown-red solution. The mixture was allowed to warm up to 0°C before being stirred at this temperature for another 1 h. A solution of the bromide 9 (2.3 g, 6.0 mmol) in dry THF (15 mL) was added at once, turning the reaction mixture light yellow brown. After 12 h of stirring at room temperature, the orange solution was quenched with MeOH (2 mL) and concentrated in vacuo. The residue was dissolved in CH₂Cl₂ and washed with water and brine, and dried (MgSO₄). Removal of the solvent gave the crude product, which was subjected to flash column chromatography (SiO₂: CH₂Cl₂/MeOH/NH₄OH 100/1/0.2) to yield the bipyridine derivative 10 (1.8 g, 66%) as a white solid. mp 172°C. δ_H (300 MHz, CDCl₃, 25°C) 1.93 (s, 6H), 2.44 (s, 6H), 3.05 (s, 4H), 6.95, 6.98, 7.19, 7.21 (AA'BB', 4H), 7.09 (dd, *J* 5, 2 Hz, 1H), 7.14 (d, *J* 4 Hz, 1H), 8.24 (d, *J* 6 Hz, 2H), 8.53 (d, *J* 5 Hz, 1H), 8.55 (d, *J* 5 Hz, 1H). δ_C (75.5 MHz, CDCl₃, 25°C) 19.1, 21.2, 36.6, 37.5, 121.4, 122.0, 124.1, 127.7, 128.3, 128.6, 129.3, 133.6, 133.7, 139.1, 140.0, 148.2, 149.0, 151.6, 156.0, 156.3. *m/z* (EIMS 70 eV) 485 (9) [M + H]⁺, 405 (9), 184 (34), 147 (64), 91 (77). (Found: C 71.65, H 6.05, N 5.70. Calc. for C₂₉H₂₉BrN₂: C 71.75, H 6.02, N 5.77%.)

4-[2-[4-[4-Hydroxymethylphenyl]-2,3,5,6-tetramethylphenyl]ethyl]-4'-methyl-2,2'-bipyridine 11

A mixture of bromide 10 (1.4 g, 2.9 mmol), the boronic acid 7 (0.91 g, 3.4 mmol), Pd(PPh₃)₄ (100 mg, 3 mol%), PhMe (20 mL), aqueous 2 M Na₂CO₃ solution (3.5 mL, 7.0 mmol), and EtOH (2 mL) was heated under reflux for 2 days. The reaction mixture was then cooled, H₂O (10 mL) was added, and the PhMe layer was separated. The aqueous

layer was extracted with EtOAc (2×20 mL) and the combined organic extracts were dried (MgSO_4), filtered, and the solvent was removed under reduced pressure. The residue was treated with TBAF (1 M solution in THF, 15 mL) at room temperature for 12 h. Solvent was removed in vacuo and the crude product was purified by flash column chromatography (SiO_2 : $\text{CH}_2\text{Cl}_2/\text{MeOH}/\text{NH}_4\text{OH}$, 100/2/0.35) to afford **11** (0.92 g, 62%) as a white solid. mp 194°C . δ_{H} (300 MHz, CDCl_3 , 25°C) 1.63 (s, 1H), 1.92 (s, 6H), 1.93 (s, 6H), 2.44 (s, 3H), 3.07 (br s, 4H), 4.77 (d, J 6 Hz, 2H), 7.07, 7.20, 7.21, 7.24 (AA'BB', 4H), 8.23 (br s, 1H), 8.27 (br s, 1H), 8.54 (d, J 4 Hz, 1H), 8.56 (d, J 4 Hz, 1H). δ_{C} (75.5 MHz, CDCl_3 , 25°C) 18.0, 18.1, 21.2, 36.7, 37.5, 65.3, 121.4, 122.1, 124.1, 124.7, 127.1, 128.4, 129.5, 129.7, 131.8, 132.0, 138.8, 139.0, 140.6, 140.8, 141.1, 142.2, 148.1, 148.2, 149.0, 151.8, 156.0, 156.2. m/z (LSIMS) 513.3 $[M + \text{H}]^+$. (Found: C 84.27, H 7.16, N 5.34. Calc. for $\text{C}_{36}\text{H}_{36}\text{N}_2\text{O}$: C 84.34, H 7.08%.)

[Ru(4,4'-dmbpy) $_2$ {4-methyl-4'-(2-(4-(4-hydroxymethylphenyl)-2,3,5,6-tetramethyl phenyl)-phenyl-ethyl)-2,2'-bipyridine}] Bis(hexafluorophosphate) 12-2PF $_6$

A mixture of $[\text{Ru}(4,4'\text{-dmbpy})_2\text{Cl}_2]^{[39]}$ (0.99 g, 1.83 mmol) and alcohol **11** (0.85 g, 1.66 mmol) in a 3/1 EtOH/ H_2O mixture (60 mL) was heated under reflux for 24 h. After removal of the solvent, the residue was purified by flash column chromatography (SiO_2 : MeOH/2 M $\text{NH}_4\text{Cl}/\text{MeNO}_2$, 7/2/1). Fractions containing the product were collected and concentrated in vacuo. The residue was treated with an excess of a 50% aqueous NH_4PF_6 solution. The red solid was filtered off, washed with H_2O , Et_2O , and dried in vacuo ($70^\circ\text{C}/0.1$ Torr) to afford the Ru complex **12-2PF $_6$** (1.4 g, 66%). mp 210°C (decomp.). δ_{H} (300 MHz, CD_3COCD_3 , 25°C) 1.78 (s, 6H), 1.89 (s, 6H), 2.51–2.56 (m, 15H), 3.14 (m, 2H), 3.25 (m, 2H), 4.72 (s, 2H), 6.96, 6.99, 7.21, 7.24 (AA'BB', 4H), 7.09, 7.12, 7.46, 7.49 (AA'BB', 4H), 7.38 (m, 6H), 7.75 (d, J 6 Hz, 1H), 7.82 (m, 5H), 8.65 (m, 6H). δ_{C} (75.5 MHz, CD_3COCD_3 , 25°C) 18.3, 21.1, 36.7, 37.6, 64.5, 125.4, 125.8, 127.5, 128.9, 129.3, 129.4, 129.6, 129.9, 130.0, 132.1, 132.3, 132.6, 132.7, 133.0, 139.3, 141.4, 141.5, 141.6, 141.8, 142.0, 150.8, 151.3, 151.5, 154.0, 157.6, 157.7. m/z (LSIMS) 1294 $[M + \text{Na}]^+$, 1127 $[M - \text{PF}_6]^+$, 981 $[M - 2\text{PF}_6]^+$. (Found: C 56.75, H 4.75, N 6.46. Calc. for $\text{C}_{60}\text{H}_{60}\text{F}_{12}\text{N}_6\text{O}_2\text{Ru}$: C 56.65, H 4.75, N 6.61%.)

[Ru(4,4'-dmbpy) $_2$ {4-methyl-4'-(2-(4-(4-bromomethylphenyl)-2,3,5,6-tetramethyl phenyl)-phenyl-ethyl)-2,2'-bipyridine}] Bis(hexafluorophosphate) 1-2PF $_6$

A solution of **12-2PF $_6$** (1.0 g, 0.79 mmol) in HBr/AcOH (12 mL, 45% w/v) was heated under reflux for 4 h. After cooling, an excess of 50% aqueous NH_4PF_6 solution was added to precipitate the product, which was then filtered off, washed with H_2O , Et_2O , and dried in vacuo ($70^\circ\text{C}/0.1$ Torr) to give the Ru-complex **1-2PF $_6$** (0.94 g, 90%), as an orange solid. mp 197°C (decomp.). δ_{H} (300 MHz, CD_3COCD_3 , 25°C) 1.79 (s, 6H), 1.89 (s, 6H), 2.51–2.56 (m, 15H), 3.14 (m, 2H), 3.25 (m, 2H), 4.76 (s, 2H), 6.97, 6.99, 7.22, 7.24 (AA'BB', 4H), 7.15, 7.17, 7.58, 7.60 (AA'BB', 4H), 7.38 (m, 6H), 7.75 (d, J 6 Hz, 1H), 7.82–7.84 (m, 5H), 8.66 (m, 6H). δ_{C} (75.5 MHz, CD_3COCD_3 , 25°C) 18.2, 21.1, 34.4, 36.7, 125.5, 125.9, 128.9, 129.3, 129.5, 129.6, 130.1, 130.2, 130.6, 132.2, 132.3, 132.6, 132.7, 132.8, 137.5, 139.3, 141.4, 141.9, 143.8, 150.9, 151.4, 151.6, 154.1, 157.7, 157.8. m/z (LSIMS) 1189 $[M - \text{PF}_6]^+$, 1045 $[M - 2\text{PF}_6]^+$. (Found: C 54.04, H 4.37, N 6.26. Calc. for $\text{C}_{60}\text{H}_{60}\text{BrF}_{12}\text{N}_6\text{P}_2\text{Ru}$: C 53.98, H 4.45, N 6.29%.)

Dumbbell Compound D-II-6PF $_6$

A mixture of **1-2PF $_6$** (316 mg, 0.25 mmol) and **2-3PF $_6$** (209 mg, 0.15 mmol) in dry MeCN (15 mL) was heated under reflux in an Ar atmosphere for 4 days. After cooling, the solvent was evaporated and the residue was purified by fresh column chromatography (SiO_2 : MeOH/2 M $\text{NH}_4\text{Cl}/\text{MeNO}_2$, 7/2/1). The fractions containing the product were combined and concentrated in vacuo, and the residue was then treated with an excess of a 50% aqueous NH_4PF_6 solution. The red solid was filtered off, washed with water and diethyl ether and dried in vacuo ($60^\circ\text{C}/0.1$ Torr) to afford the dumbbell-shaped compound **D-II-6PF $_6$**

(241 mg, 57%). mp $220\text{--}223^\circ\text{C}$ (decomp.). δ_{H} (500 MHz, CD_3COCD_3 , 25°C) 1.22 (t, J 8 Hz, 3H), 1.32 (s, 18H), 1.82 (s, 6H), 1.90 (s, 6H), 2.40 (s, 3H), 2.42 (s, 3H), 2.54 (s, 3H), 2.56 (s, 3H), 2.57–2.58 (m, 9H), 2.63 (q, J 8 Hz, 2H), 3.10–3.21 (m, 4H), 3.22–3.29 (m, 2H), 3.95 (m, 2H), 4.17 (m, 2H), 4.28 (m, 2H), 5.11 (t, J 5 Hz, 2H), 5.17 (t, J 8 Hz, 2H), 5.26 (t, J 8 Hz, 2H), 6.32 (s, 2H), 6.87 (d, J 9 Hz, 2H), 7.01 (d, J 8 Hz, 2H), 7.10–7.17 (m, 10H), 7.28 (d, J 8 Hz, 2H), 7.29–7.34 (m, 6H), 7.34–7.40 (m, 6H), 7.77 (d, J 6 Hz, 2H), 7.81–7.87 (m, 6H), 8.21 (d, J 6 Hz, 1H), 8.26 (d, J 6 Hz, 1H), 8.65–8.69 (m, 6H), 8.87 (d, J 7 Hz, 2H), 8.91 (d, J 7 Hz, 2H), 9.20 (d, J 7 Hz, 1H), 9.22 (d, J 7 Hz, 1H), 9.28 (s, 1H), 9.31 (s, 1H), 9.45 (d, J 7 Hz, 2H), 9.64 (d, J 7 Hz, 2H). δ_{C} (125 MHz, CD_3COCD_3 , 25°C) 14.8, 16.2, 17.2, 17.3, 20.1, 30.6, 32.6, 33.8, 35.7, 36.6, 58.4, 58.6, 61.6, 63.0, 64.6, 67.0, 68.8, 69.4, 113.1, 124.1, 124.4, 124.8, 126.7, 127.0, 127.5, 127.6, 127.7, 127.9, 128.3, 128.6, 129.1, 129.4, 130.4, 130.5, 130.6, 131.1, 131.4, 131.8, 137.3, 138.0, 138.4, 139.5, 139.9, 140.3, 141.1, 141.4, 142.7, 143.3, 144.2, 144.5, 144.6, 146.0, 146.1, 146.3, 146.5, 148.2, 149.9, 150.4, 150.6, 152.0, 152.3, 153.1, 156.6, 156.7, 156.8. m/z (FAB) 2622 $[M - \text{PF}_6]^+$, 2474 $[M - 2\text{PF}_6]^+$, 2329 $[M - 3\text{PF}_6]^+$, 2184 $[M - 4\text{PF}_6]^+$.

Bistable [2]Rotaxane BR-II-6PF $_6$

A solution of dumbbell-shaped compound **D-II-6PF $_6$** (177 mg, 0.06 mmol) and bis-p-phenylene[34]crown-10 (206 mg, 0.38 mmol) in dry MeCN (2 mL) was stirred at 50°C for 4 days. The solvent was removed in vacuo and the residue was purified by flash column chromatography (SiO_2 : MeOH/2 M $\text{NH}_4\text{Cl}/\text{MeNO}_2$, 7/2/1) to give, after counterion exchange (50% aqueous solution NH_4PF_6), the bistable [2]rotaxane compound **BR-II-6PF $_6$** (109 mg, 52%). mp $187\text{--}191^\circ\text{C}$ (decomp.). δ_{H} (500 MHz, CD_3CN , 25°C) 1.15 (t, J 8 Hz, 3H), 1.24 (s, 18H), 1.74 (s, 6H), 1.87 (s, 6H), 2.22 (s, 3H), 2.27 (s, 3H), 2.43 (s, 3H), 2.47 (s, 3H), 2.48–2.50 (m, 9H), 2.56 (q, J 8 Hz, 2H), 2.89 (m, 2H), 3.04–3.15 (m, 4H), 3.55–3.59 (m, 6H), 3.67–3.80 (m, 20H), 4.03–4.05 (m, 2H), 4.05–4.07 (m, 2H), 4.67–4.69 (m, 4H), 4.77–4.80 (m, 2H), 4.83–4.87 (m, 2H), 5.97 (s, 2H), 6.12 (s, 8H), 6.80 (d, J 9 Hz, 2H), 6.90 (d, J 8 Hz, 2H), 7.08–7.18 (m, 18H), 7.27–7.36 (m, 8H), 7.48 (d, J 6 Hz, 2H), 7.49–7.51 (m, 4H), 7.76 (d, J 6 Hz, 2H), 7.81 (d, J 6 Hz, 2H), 7.88–7.93 (m, 6H), 8.25–8.30 (m, 6H), 8.70 (d, J 7 Hz, 1H), 8.76–8.82 (m, 3H), 8.86–8.90 (m, 4H), 9.04 (d, J 7 Hz, 2H). m/z (FAB) 3012 $[M - 2\text{PF}_6]^+$, 2867 $[M - 3\text{PF}_6]^+$, 2721 $[M - 4\text{PF}_6]^+$, 1506 $[M - 2\text{PF}_6]^{2+}$.

Electrochemical Measurements

Electrochemical experiments were carried out in argon-purged MeCN solution at room temperature with an EcoChemie Autolab 30 multi-purpose instrument interfaced to a personal computer. In the cyclic voltammetry (CV) and differential pulse voltammetry (DPV) experiments, the working electrode was a glassy carbon electrode (0.08 cm^2 , Amel); its surface was routinely polished with a 0.05 μm alumina-water slurry on a felt surface, immediately before use. In all cases, the counter electrode was a Pt wire and the reference was a saturated calomel electrode (SCE) separated with a fine glass frit. The concentration of the compounds examined was 5.0×10^{-4} mol L^{-1} ; 0.05 mol L^{-1} tetraethylammonium hexafluorophosphate was added as the supporting electrolyte. Cyclic voltammograms were obtained as sweep rates of 20, 50, 200, 500, and 1000 mV s^{-1} ; DPV experiments were performed with a scan rate of 20 mV s^{-1} and a pulse height of 75 mV, and a duration of 40 ms. In order to resolve overlapping peaks, DPV experiments with a scan rate of 4 mV s^{-1} and a pulse height of 10 mV were also carried out. Ferrocene was present as an internal standard. The experimental error was estimated to be ± 5 mV.

Photophysical and Photochemical Experiments

Measurements were carried out at 298 K on MeCN (Merck Uvasol) solutions with concentrations ranging from 5×10^{-6} to 10^{-4} mol L^{-1} . UV-Vis absorption spectra were recorded on air-equilibrated solutions with a Perkin Elmer $\lambda 40$ spectrophotometer. Uncorrected luminescence spectra were obtained with a Perkin Elmer LS-50 or Edinburgh Instruments FLS920 spectrofluorimeter, equipped with a Hamamatsu

R928 phototube, on solutions degassed with at least four freeze-pump-thaw cycles and sealed under vacuum (8×10^{-9} bar). Luminescence quantum yields were determined by the optically dilute method using $[\text{Ru}(\text{bpy})_3]^{2+}$ in air-equilibrated water ($\Phi = 0.028$) as a standard.^[41] Low-temperature (77 K) luminescence spectra were obtained on a butyronitrile (Fluka) rigid matrix. Photochemical experiments were carried out by irradiation of degassed solutions (see above) at 436 nm with a Hg medium pressure lamp (Helios Italquartz, 150 W); the exciting wavelength was isolated by means of an interference filter. Luminescence lifetimes were measured by time-correlated single-photon counting with an Edinburgh Instruments FLS920 equipment. The exciting light ($\lambda = 300$ nm) was produced by a gas arc lamp (model nF900, deuterium filled), delivering pulses of ~ 1 ns (fwhm), and the detector was a cooled Hamamatsu R928 photomultiplier. Nanosecond transient absorption experiments were performed by exciting the sample at $\lambda = 532$ nm (obtained by frequency doubling) with 10 ns (fwhm) pulses of a Continuum Surelite I-10 Nd:Yag laser (10 Hz repetition rate) and using a pulsed 150 W Xe lamp, perpendicular to the laser beam, as a probing light. The Xe lamp was equipped with an Applied Photophysics power supply (Model 40) and pulsing unit (Model 410, 2 ms pulses). A shutter (Oriol 71445), placed between the lamp and the sample, was opened for 100 ms to prevent phototube fatigue and photodecomposition. Suitable pre- and post-cutoff and bandpass filters were also used to avoid photodecomposition and interferences from scattered light. The light was collected in a PTI monochromator (model 01-001), detected by a Hamamatsu R928 tube, and recorded on a Tektronix TDS380 (400 MHz) digital oscilloscope connected to a PC. Synchronous timing of the system was achieved by means of a built-in-house digital logic circuit. The absorption transient decays were plotted as $\Delta A = \log(I_0/I_t)$ versus time, where I_0 and I_t were the probing the light intensities before the laser pulse and after delay t , respectively. Each decay was obtained by averaging ten pulses. Transient absorption spectra were obtained from the decays measured at various wavelengths, by sampling the absorbance changes at constant delay time.

Acknowledgments

A part of this research was supported by a National Science Foundation (NSF) Nanoscale Interdisciplinary Research Team fund (NIRT ECS-0103559), an Office of Naval Research grant (contract number N00014-00-1-0216), an NSF Equipment Grant (CHE-9974928), an NIH Shared Instrument Grant (S10RR1S9S2), and the Center for Cell Mimetic Space Exploration (CMISE) — a NASA University Research, Engineering, and Technology Institute (URETI) award (number NCC2-1364). The European Union is gratefully acknowledged for support under the auspices of the Molecular-Level Devices and Machines RTN Network, the Biomach STREP project, and a Marie Curie Individual Fellowship to M.C.-L. The Italian authors complain that they cannot thank any Italian agency for financial support.

References

- [1] V. Balzani, A. Credi, F. M. Raymo, J. F. Stoddart, *Angew. Chem. Int. Ed.* **2000**, *39*, 3348. doi:10.1002/1521-3773(20001002)39:19<3348::AID-ANIE3348>3.0.CO;2-X
- [2] J.-P. Collin, C. O. Dietrich-Buchecker, P. Gaviña, M. C. Jimenez-Molero, J.-P. Sauvage, *Acc. Chem. Res.* **2001**, *34*, 477. doi:10.1021/AR0001766
- [3] *Molecular Switches* (Ed. B. L. Feringa) **2001** (Wiley-VCH: Weinheim).
- [4] V. Balzani, A. Credi, M. Venturi, *Molecular Devices and Machines — A Journey into the Nano World* **2003** (Wiley-VCH: Weinheim).
- [5] A. H. Flood, R. J. A. Ramirez, W. Q. Deng, R. P. Muller, W. A. Goddard, J. F. Stoddart, *Aust. J. Chem.* **2004**, *57*, 301. doi:10.1071/CH03307
- [6] Special issue on molecular machines: *Top. Curr. Chem.* **2005**, *262*.
- [7] D. S. Goodsell, *Nanobiotechnology: Lessons from Nature* **2004** (Wiley: New York, NY).
- [8] M. Schliwa, G. Woehlke, *Nature* **2003**, *422*, 759. doi:10.1038/NATURE01601
- [9] G. Steinberg-Yfrach, J. L. Rigaud, E. N. Durantini, A. L. Moore, D. Gust, T. A. Moore, *Nature* **1998**, *392*, 479. doi:10.1038/33116
- [10] I. M. Bennett, H. M. V. Farfano, F. Bogani, A. Primak, P. A. Liddell, L. Otero, L. Sereno, J. J. Silber, A. L. Moore, T. A. Moore, D. Gust, *Nature* **2002**, *420*, 398. doi:10.1038/NATURE01209
- [11] P. Thordarson, E. J. A. Bijsterveld, A. E. Rowan, R. J. M. Nolte, *Nature* **2003**, *424*, 915. doi:10.1038/NATURE01925
- [12] A. Kocer, M. Walko, W. Meijberg, B. L. Feringa, *Science* **2005**, *309*, 755. doi:10.1126/SCIENCE.1114760
- [13] A. M. Brouwer, C. Frochot, F. G. Gatti, D. A. Leigh, L. Mottier, F. Paolucci, S. Roffia, G. W. H. Wurpel, *Science* **2001**, *291*, 2124. doi:10.1126/SCIENCE.1057886
- [14] D. A. Leigh, J. K. Y. Wong, F. Dehez, F. Zerbetto, *Nature* **2003**, *424*, 174. doi:10.1038/NATURE01758
- [15] C. A. Stanier, S. J. Alderman, T. D. W. Claridge, H. L. Anderson, *Angew. Chem. Int. Ed.* **2002**, *41*, 1769. doi:10.1002/1521-3773(20020517)41:10<1769::AID-ANIE1769>3.0.CO;2-N
- [16] D. H. Qu, Q. C. Wang, H. Tian, *Angew. Chem. Int. Ed.* **2005**, *44*, 5296. doi:10.1002/ANIE.200501215
- [17] J. D. Badjic, V. Balzani, A. Credi, S. Silvi, J. F. Stoddart, *Science* **2004**, *303*, 1845. doi:10.1126/SCIENCE.1094791
- [18] E. Katz, O. Lioubashevsky, I. Willner, *J. Am. Chem. Soc.* **2004**, *126*, 15520. doi:10.1021/JA045465U
- [19] P. Mobian, J.-M. Kern, J.-P. Sauvage, *Angew. Chem. Int. Ed.* **2004**, *43*, 2392. doi:10.1002/ANIE.200352522
- [20] M. C. Jimenez, C. Dietrich-Buchecker, J.-P. Sauvage, *Angew. Chem. Int. Ed.* **2000**, *39*, 3284. doi:10.1002/1521-3773(20000915)39:18<3284::AID-ANIE3284>3.0.CO;2-7
- [21] T. D. Nguyen, H.-R. Tseng, P. C. Celestre, A. H. Flood, Y. Liu, J. F. Stoddart, J. I. Zink, *Proc. Natl. Acad. Sci. USA* **2005**, *102*, 10029. doi:10.1073/PNAS.0504109102
- [22] W. S. Jeon, E. Kim, Y. H. Ko, I. H. Hwang, J. W. Lee, S. Y. Kim, H. J. Kim, K. Kim, *Angew. Chem. Int. Ed.* **2005**, *44*, 87. doi:10.1002/ANIE.200461806
- [23] Y. Liu, A. H. Flood, P. A. Bonvallet, S. A. Vignon, B. H. Northrop, H.-R. Tseng, J. O. Jeppesen, T. J. Huang, B. Brough, M. Baller, S. Magonov, S. D. Solares, W. A. Goddard, C. M. Ho, J. F. Stoddart, *J. Am. Chem. Soc.* **2005**, *127*, 9745. doi:10.1021/JA051088P
- [24] P. R. Ashton, R. Ballardini, V. Balzani, A. Credi, R. Dress, E. Ishow, C. J. Kleverlaan, O. Kocian, J. A. Preece, N. Spencer, J. F. Stoddart, M. Venturi, S. Wenger, *Chem. Eur. J.* **2000**, *6*, 3558. doi:10.1002/1521-3765(20001002)6:19<3558::AID-CHEM3558>3.0.CO;2-M
- [25] V. Balzani, M. Clemente-León, A. Credi, B. Ferrer, M. Venturi, A. H. Flood, J. F. Stoddart, *Proc. Natl. Acad. Sci. USA* **2006**, *103*, 1178. doi:10.1073/PNAS.0509011103
- [26] F. M. Raymo, K. N. Houk, J. F. Stoddart, *J. Am. Chem. Soc.* **1998**, *120*, 9318. doi:10.1021/JA9806229
- [27] A. Juris, V. Balzani, F. Barigelletti, S. Campagna, P. Belser, A. von Zelewsky, *Coord. Chem. Rev.* **1988**, *84*, 85. doi:10.1016/0010-8545(88)80032-8
- [28] H. Sun, A. Yoshimura, M. Z. Hoffman, *J. Phys. Chem.* **1994**, *98*, 5058, and references therein. doi:10.1021/J100070A019
- [29] P. R. Ashton, R. Ballardini, V. Balzani, M. Belohradsky, M. T. Gandolfi, D. Philp, L. Prodi, F. M. Raymo, M. Reddington, N. Spencer, J. F. Stoddart, M. Venturi, D. J. Williams, *J. Am. Chem. Soc.* **1996**, *118*, 4931. doi:10.1021/JA954334D
- [30] E. H. Yonemoto, G. B. Saupe, R. H. Schmehl, S. M. Hubig, R. L. Riley, B. L. Iveson, T. E. Mallouk, *J. Am. Chem. Soc.* **1994**, *116*, 4786. doi:10.1021/JA00090A026

- [31] L. A. Kelly, M. A. J. Rodgers, *J. Phys. Chem.* **1995**, *99*, 13132. doi:10.1021/J100035A015
- [32] P. R. Ashton, R. Ballardini, V. Balzani, E. C. Constable, A. Credi, O. Kocian, S. J. Langford, J. A. Preece, L. Prodi, E. R. Schofield, N. Spencer, J. F. Stoddart, S. Wenger, *Chem. Eur. J.* **1998**, *4*, 2413. doi:10.1002/(SICI)1521-3765(19981204)4:12<2413::AID-CHEM2413>3.0.CO;2-A
- [33] N. A. McAskill, *Aust. J. Chem.* **1984**, *37*, 1579. doi:10.1071/CH9841579
- [34] T. Watanabe, K. Honda, *J. Phys. Chem.* **1982**, *86*, 2617. doi:10.1021/J100211A014
- [35] M. Z. Hoffman, F. Bolletta, L. Moggi, G. L. Hug, *J. Phys. Chem. Ref. Data* **1989**, *18*, 219.
- [36] J. Rebek, Jr, T. Costello, R. Wattlely, *J. Am. Chem. Soc.* **1985**, *107*, 7487. doi:10.1021/JA00311A044
- [37] J. L. Sessler, B. Wang, A. Harriman, *J. Am. Chem. Soc.* **1995**, *117*, 704. doi:10.1021/JA00107A014
- [38] F. Jannasch, *Z. Chem.* **1870**, 162.
- [39] P. Lay, A. M. Sargeson, H. Taube, *Inorg. Synth.* **1986**, *24*, 292.
- [40] D. D. Perrin, W. F. L. Armarego, *Purification of Laboratory Chemicals* **1989** (Pergamon: Oxford).
- [41] M. Montalti, A. Credi, L. Prodi, M. T. Gandolfi, *Handbook of Photochemistry*, 3rd edn **2006**, Ch. 10 (CRC Press: Boca Raton, FL).